Biochemistry and Biophysics Reports 15 (2018) 107–114

Contents lists available at ScienceDirect

Biochemistry and Biophysics Reports

journal homepage: www.elsevier.com/locate/bbrep

# Autophagy-disrupted LC3 abundance leads to death of supporting cells of human oocytes

Woojin Kang[a,b,1], Eri Ishida[a,1], Kenji Yamatoya[c,1], Akihiro Nakamura[b,d], Mami Miyado[e], Yoshitaka Miyamoto[b], Maki Iwai[b,d], Kuniko Tatsumi[a], Takakazu Saito[a], Kazuki Saito[a], Natsuko Kawano[f], Toshio Hamatani[d], Akihiro Umezawa[b], Kenji Miyado[b,*], Hidekazu Saito[a,*]

[a] Department of Perinatal Medicine and Maternal Care, National Center for Child Health and Development, 2-10-1 Okura, Setagaya, Tokyo 157-8535, Japan
[b] Department of Reproductive Biology, National Research Institute for Child Health and Development, 2-10-1 Okura, Setagaya, Tokyo 157-8535, Japan
[c] Department of Applied Biological Science, Tokyo University of Science, 2641 Yamazaki, Noda, Chiba 278-8510, Japan
[d] Department of Obstetrics and Gynecology, Keio University School of Medicine, 35 Shinanomachi, Shinjuku, Tokyo 160-8582, Japan
[e] Department of Molecular Endocrinology, National Research Institute for Child Health and Development, 2-10-1 Okura, Setagaya, Tokyo 157-8535, Japan
[f] Department of Life Sciences, School of Agriculture, Meiji University, 1-1-1 Higashimita, Kawasaki, Kanagawa 214-8571, Japan

ARTICLE INFO

*Keywords:*
Human granulosa cells
Autophagy
LC3
ATG7
Cell death
Cumulus cells

ABSTRACT

Autophagic recycling of cell parts is generally termed as the opposite of cell death. Here, we explored the relation between cell death and autophagy by examining granulosa cell layers that control oocyte quality, which is important for the success of fertilization. Granulosa cell layers were collected from infertile women and morphologically divided into four types, viz., mature (MCCs), immature (ICCs), and dysmature cumulus cells (DCCs), and mural granulosa cells (MGCs). Microtubule-associated protein light chain 3 (LC3), which is involved in autophagosome formation, was expressed excessively in DCCs and MGCs, and their chromosomal DNA was highly fragmented. However, autophagy initiation was limited to MGCs, as indicated by the expression of membrane-bound LC3-II and autophagy-related protein 7 (ATG7), an enzyme that converts LC3-I to LC3-II. Although pro-LC3 was accumulated, autophagy was disabled in DCCs, resulting in cell death. Our results suggest the possibility that autophagy-independent accumulation of pro-LC3 proteins leads to the death of human granulosa cells surrounding the oocytes and presumably reduces oocyte quality and female fertility.

## 1. Introduction

In mammals, ovarian follicles consist of three types of layered somatic cells, viz., theca, granulosa, and cumulus cells (CCs), in addition to oocytes [1,2]. When each ovarian follicle matures, CCs differentiate from multiple layers of granulosa cells and surround a single oocyte. Despite their morphologically similarity, CCs play a critical role in the formation of fertilization-competent oocytes.

Macroautophagy (hereafter autophagy) often occurs prior to apoptosis [3]. Membrane vesicles, termed as autophagosomes, enclose a part of the cytoplasm and organelles, and its contents are degraded by the unification of lysosome and autophagosome (Fig. 1A). Autophagy governs both apoptosis and clearance of cellular waste, thereby maintaining cellular homeostasis. LC3, a mammalian homologue of yeast Atg8 (Aut7/Apg8), localizes to the autophagosomal membranes after posttranslational modifications [4]. Autophagy-related genes (Atgs) participate in autophagosome formation, and LC3 is a convincing marker of initiation of autophagosome formation. The C-terminus of LC3 is cleaved by Atg4 protease, which generates cytosolic LC3-I; LC3-I is conjugated to phosphatidylethanolamine (PE) and lipidated in a ubiquitin-like reaction that requires Atg7, one of the E1-like enzymes. This lipidated product, LC3-II, is bound to the membrane of autophagosomes. Finally, aging cells and damaged organelles are degraded by the fusion of autophagosomes with lysosomes [5].

Autophagy has been investigated with respect to reproduction and early embryogenesis. Interaction between apoptosis and autophagy promotes the formation of corpus luteum and the survival of androgen-secreting cells [6]. Autophagy functions during gametogenesis because autophagy is indispensable to synthesize a new zygote protein from resolvents of the maternal proteins [7,8]. However, in fish, apoptosis occurs in the follicular atresia simultaneously with autophagy [9]. Apoptosis is also known to occur in both human cumulus and granulosa

* Corresponding authors.
*E-mail addresses:* miyado-k@ncchd.go.jp (K. Miyado), saitou-hi@ncchd.go.jp (H. Saito).
[1] Authors equally contributed to this work.

https://doi.org/10.1016/j.bbrep.2018.08.002
Received 23 March 2018; Received in revised form 27 June 2018; Accepted 6 August 2018
Available online 21 August 2018
2405-5808/ © 2018 The Authors. Published by Elsevier B.V. This is an open access article under the CC BY-NC-ND license (http://creativecommons.org/licenses/BY-NC-ND/4.0/).

A

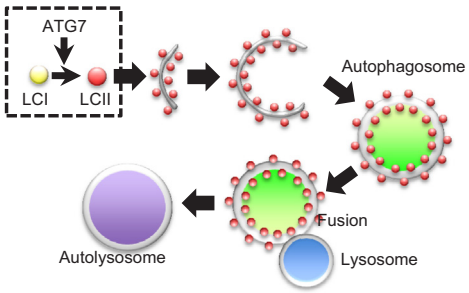


B

| | |
|---|---|
| Number of patients | 9 |
| Age (years) | 38.8 ± 1.3 |
| Day3 FSH (mIU/ml) | 4.6 ± 0.4 |
| Day3 LH (mIU/ml) | 2.8 ± 0.6 |
| Day3 estradiol (pg/ml) | 31.2 ± 4.8 |
| Day of hCG estradiol (pg/ml) | 3266.7 ± 549.2 |
| Day of hCG progesterone (ng/ml) | 0.5 ± 0.1 |
| Day of hCG FSH (mIU/ml) | 15.0 ± 1.6 |
| Day of hCG LH (mIU/ml) | 2.1 ± 0.4 |
| Ampoules of gonadotropin used* | 21.4 ± 1.7 |
| Days of stimulation | 13.0 ± 0.5 |
| Number of follicles aspirated | 14.2 ± 1.9 |
| Number of oocytes retrieved | 12.6 ± 1.5 |
| Number of mature COCs** | 6.2 ± 1.2 |
| Number of immature COCs | 4.1 ± 0.6 |
| Number of dysmature COCs | 2.2 ± 0.4 |
| Number of embryos fertilized | 6.6 ± 1.5 |

*1 ampoule = 75IU
**COCs: Cumulus-oocyte-complex

**Fig. 1. General scheme of autophagy and clinical data of the patients**. **A**, Scheme of autophagy and participation of ATG7 in LC3 activation during autophagy. **B**, Clinical demographic data of the patients (mean ± SE).

A

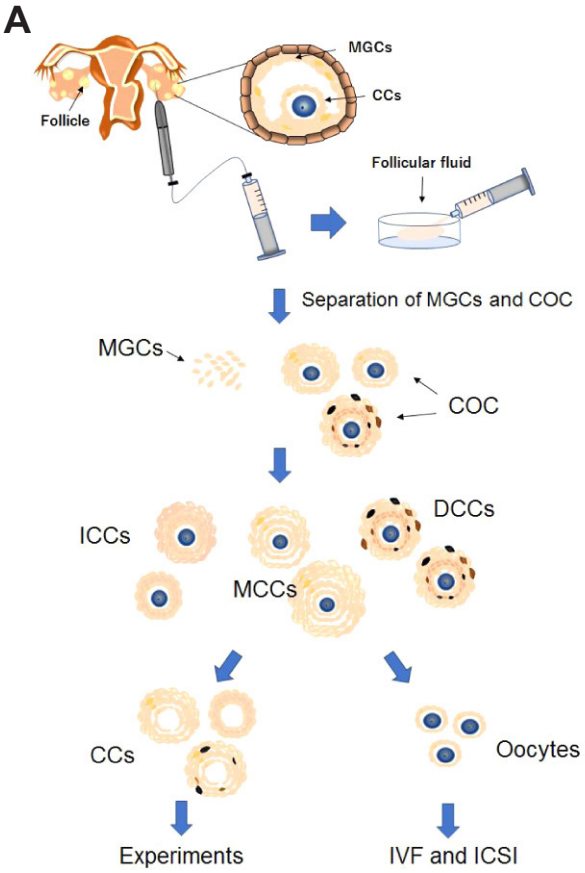


B

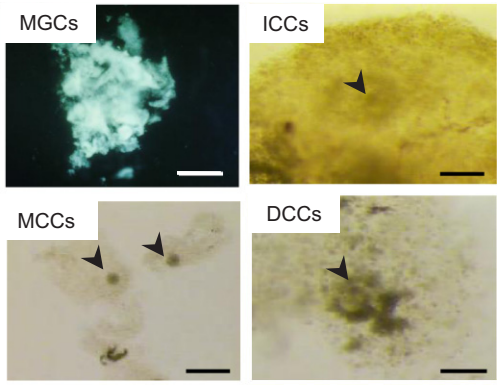


C

| | Total number of oocyte | Number of fertilized oocytes | Fertilized oocyte (%) |
|---|---|---|---|
| ICCs | 837 | 450 | 53.8 |
| MCCs | 1359 | 825 | 60.7 |
| DCCs | 321 | 109 | 34.0* |

* Significant difference among groups
(ICCs v.s. DCCs, $p<0.001$; MCCs v.s. DCCs, $p<0.001$)

**Fig. 2. Flow chart for collecting samples and fertilization rate by maturity of cumulus cells**. **A**, Flow chart of collecting cumulus cells (CCs) from cumulus-oocyte complex (COC). COCs were retrieved from stimulated follicle by hormones. Human granulosa cells (MGCs) and COCs were isolated from follicular aspirates. The maturity of COCs was evaluated based on morphologic criteria. Evaluated CCs were physically detached from COCs. Obtained CCs were used in experiments and oocytes were used for ART by IVF or ICSI. **B**, Classification of MGCs and CCs. The cells were divided into four cell types, viz., MGCs, ICCs, MCCs, and DCCs. Arrowheads indicate oocytes. Scale bars, 100 μm. **C**, Fertilization rate of oocytes separated from ICCs, MCCs, and DCCs. Table shows general fertilizatuion rate using oocytes that were separated based on maturity of CCs.

cells; however, its connection with autophagy in mammalian reproduction remains unknown. In this study, we explored the role of autophagy in maintaining CC quality.

## 2. Materials and methods

### 2.1. Patients and follicle stimulation protocol

Human granulosa cells [cumulus and mural granulosa cells (MGCs)] were obtained from patients treated with assisted reproductive

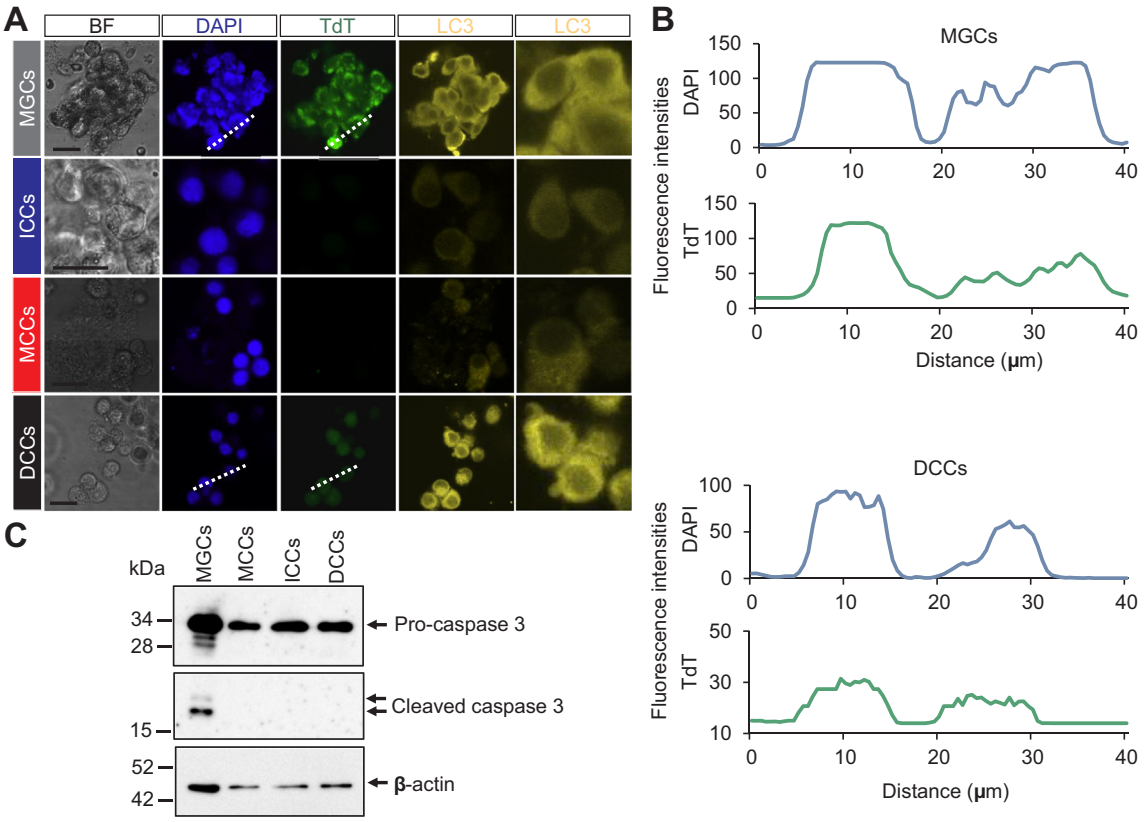


**Fig. 3. Expression of LC3 and detection of apoptosis**. **A**, Immunostaining. Immunostaining of LC3; TUNEL assay was performed, and fluorescent images were captured. Green and yellow signals represented TUNEL/488 and LC3 staining, respectively. Blue signals represented DAPI staining. Scale bars, 20 μm. **B**, The fluorescence intensity profiles of DAPI- and TdT-stained areas in cells shown in A. Fluorescence intensities were measured along with white dotted lines. **C**, Immunoblotting with anti-caspase 3 polyAb. β-actin was immunoblotted as an internal control.

technologies (ART) at National Center for Child Health and Development, Japan. All patients gave informed consent for this study. The follicular stimulation protocol has been described previously [10]. The follicles were stimulated with recombinant follicle stimulating hormone (FSH; Follistim, Organon, Tokyo, Japan) according to the GnRH agonist long protocol, and ovulation was induced by administration of 10,000 IU human chorionic gonadotropin (hCG) (Gonadotropin; Aska, Tokyo, Japan) when the leading follicle was 18 mm in diameter. Cumulus-oocyte complex (COCs) were retrieved using an 18-G needle guided by transvaginal sonography from 35 to 36 h after the hCG injection.

### 2.2. Cumulus and MGC preparation

Isolated COCs were washed twice in Sydney IVF fertilization medium (COOK Medical, Brisbane, Australia). CCs were then physically detached from COCs using 27-G fine needles (Terumo, Kanagawa, Japan). Just before detaching the CCs, the maturity of COCs was evaluated based on the following morphologic criteria: [I], complete expansion of cumulus with visible halo (mature); [II], incomplete expansion of cumulus without halo (immature); and [III], incomplete or complete expansion and dissociation of cumulus with dark spots (dysmature). In addition, MGCs were isolated from follicular aspirates. For immunofluorescence, a portion of MGCs and CCs was transferred into a dish (Falcon 353001) and washed three times with 0.1% bovine serum albumin (BSA) in phosphate-buffered saline (PBS). Then, the samples were fixed in 4% formaldehyde in 0.1% BSA in PBS for 30 min at room temperature (RT), washed three times with 0.1% BSA in PBS, placed on glass slides, air-dried, and stored at 4 °C until use.

### 2.3. In vitro fertilization (IVF) and intracytoplasmic sperm injection (ICSI)

The IVF procedure used in this study has been previously described [10]. Semen was collected by masturbation and, washed, and motile sperm were separated using a 30–60 min swim-up period. IVF was performed by incubating each oocyte with 50–100 × $10^3$ motile sperm for 5–6 h. When there was evidence of male factor infertility, ICSI was performed according to a previous report [10]. Oocytes were examined using a dissecting microscope 16–18 after insemination or ICSI. The presence of two pronuclei was taken as evidence of successful fertilization.

### 2.4. Antibodies

Human anti-LC3 polyclonal antibody (polyAb) was purchased from MBL (AB843283, Aichi, Japan), and anti-β-tubulin monoclonal antibody (mAb) was purchased from Sigma-Aldrich (St Louis, MO). Human anti-capase 3 and ATG7 polyAbs were purchased from Abcam (ab184787, Cambridge, UK) and ProSci Inc. (AB735306, Poway, CA). Anti-glyceraldehyde-3-phosphate dehydrogenase (GAPDH) mAb was purchased from Wako Pure Chemical Industries (016-25523, Osaka, Japan). Alexa 488-conjugated IgG (Thermo Fisher Scientific Inc., Waltham, MA) was used as a secondary antibody. Horseradish peroxidase-conjugated secondary antibodies (Sigma-Aldrich, St Louis, MO) were used for immunoblotting. Nuclei were counterstained with 4′,6-diamidino-2-phenylindole (DAPI; Wako Pure Chemical Industries, Osaka, Japan).

### 2.5. Immunoblotting

Human granulosa cells were separated from the oocytes in COCs, lysed, and denatured in Laemmli's SDS sample buffer, containing 2% SDS, 62.5 mM Tris-HCl (pH 6.8), 0.005% bromophenol blue, and 7% glycerol, boiled at 95 °C for 10 min, and subjected to SDS-PAGE on 15%

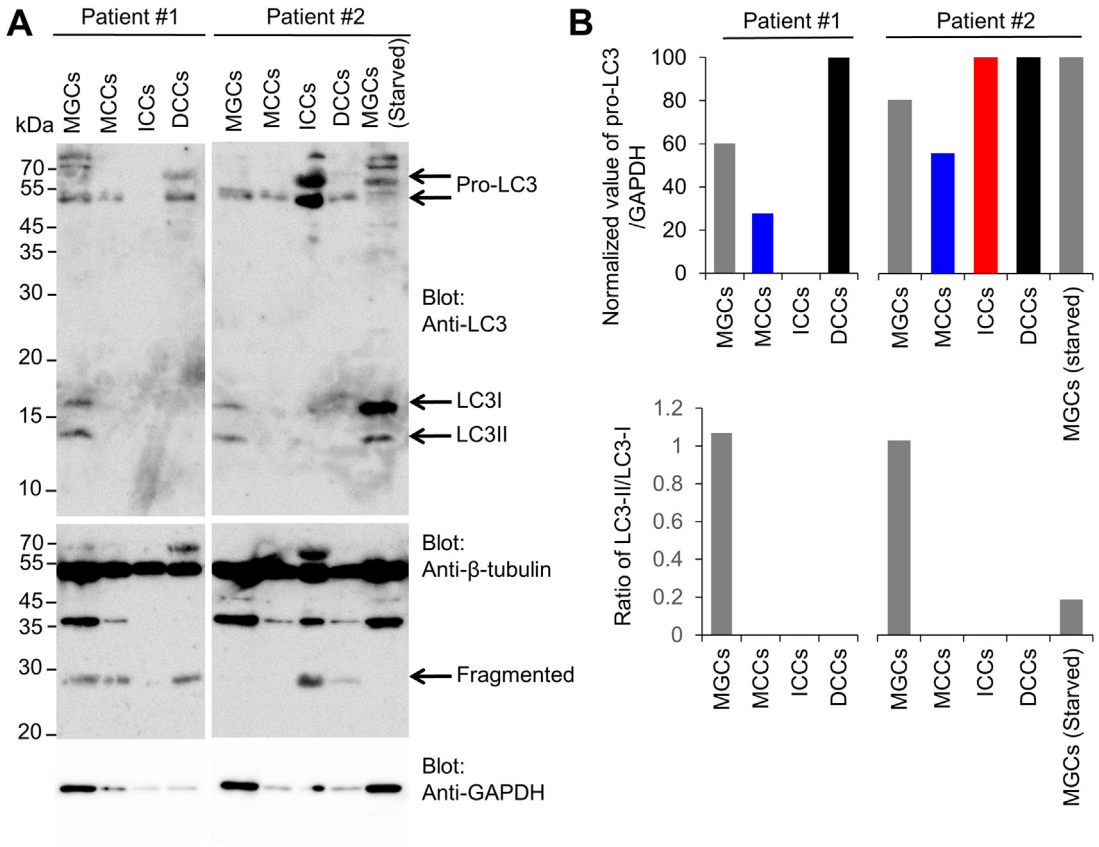


**Fig. 4. Detection of LC3-I and -II proteins**. **A**, Detection of LC3-I and -II proteins. MGCs and CCs (ICCs, MCCs, and DCCs) of patient #1 and #2 were subjected to western blot analysis. The corresponding bands that represented LC3-I, -II, β-tubulin, and fragmented β-tubulin are indicated. β-tubulin and GAPDH were used to normalize the results. MGCs (Starved; lane 5 of patient #1) were incubated with serum free medium for 24 h to increase the expression of LC3 proteins. **B**, Quantification of pro-LC3 (upper graph) and the ratio of LC3-II/LC3-I proteins (lower graph). The amounts of pro-LC3 proteins were estimated densitometrically and normalized to those of GAPDH. The amounts of pro-LC3 in DCCs of patient #1 and #2 were set to 100. In the lower graph, the amounts of LC3-II proteins were estimated densitometrically and normalized with those of LC3-I proteins.

acrylamide gels prior to immunoblotting. Immune complexes of anti-human caspase 3 (ab184787, Abcam, Cambridge, UK), LC3 (AB843283, MBL, Nagoya, Japan), and ATG7 (AB735306, ProSci Inc., Poway, CA) polyAbs of interest were determined by enzyme-linked color development with horseradish peroxidase conjugated to the secondary antibodies (Sigma-Aldrich, St. Louis, MO).

### 2.6. Immunofluorescence

MGCs and cumulus cells prepared as described above were permeabilized with 0.5% Triton X-100 in PBS for 5 min at RT and blocked with 1% BSA and 0.1% Tween 20 in PBS for 1 h at RT. The samples were incubated overnight at 4 °C with anti-human LC3 (AB843283, MBL, Nagoya, Japan) and ATG7 (AB735306, ProSci Inc., Poway, CA) poly Abs, which were prepared as a 1:500 dilution in Dako antibody diluents (Dako, Carpinteria, CA). The complexes were then washed three times with 0.1% Tween 20 in PBS and visualized with anti-rabbit IgG conjugated with Alexa546 or Alexa488 diluted to 1:1000 in Dako antibody diluents for 1 h at RT. On the other hand, to detect DNA fragmentation, we performed terminal deoxynucleotidyl transferase (TdT)-mediated dUTP nick end labeling (TUNEL) staining using TUNEL staining kit (Roche, CA). The permeabilized samples were incubated with overnight at 4 °C with dUTP-biotin. The complexs were washed three times with 0.1% Tween 20 in PBS and visualized with avidin-Alexa488. In addition, lysosomes were stained with LysoTracker Green DND-26 (Invitrogen, Molecular probes, Eugene, OR) to a final concentration of 5 nM and incubated for 20 min at RT. To count the number of cells, 10 mM Hoechst33342 was loaded with 0.1% Tween 20 in PBS during treatment with the secondary antibody. The samples were then washed three times with 0.1% Tween 20 in PBS, immersed in Vectashield (Vector Laboratories Inc., Burlingame, CA), and covered with coverslips. Microphotographs were captured using a fluorescence microscope (BX-51; Olympus, Tokyo, Japan) equipped with a computational CCD camera (DP70; Olympus). Photographs captured from five to ten different areas of each sample were analyzed with Olympus DP Controller and DP Manager (Olympus, Tokyo, Japan). To estimate ATG7 expression and abundance of lysosomes, fluorescent intensities were quantified by using the BZ-analyzer software (Keyence Japan, Osaka, Japan). In each experiment, at least 300 cells were measured in randomly selected microscopic fields.

### 2.7. Statistical analysis

Significant differences (*P*-values) were calculated using Student's *t*-test and the chi-square test, and statistical significance was set at $P < 0.05$. Results were expressed as mean ± SE.

## 3. Results

### 3.1. Characteristics and outcomes of in vitro fertilization–embryo transfer (IVF–ET)

The characteristics of the group undergoing IVF–ET are shown in Fig. 1B. We representatively performed nine IVF–ET cycles, with one embryo transfer cycle. The mean age of the women was 38.8 ± 1.3 years, and the serum FSH level on day 3 was normal (4.6 ± 0.4 mIU/

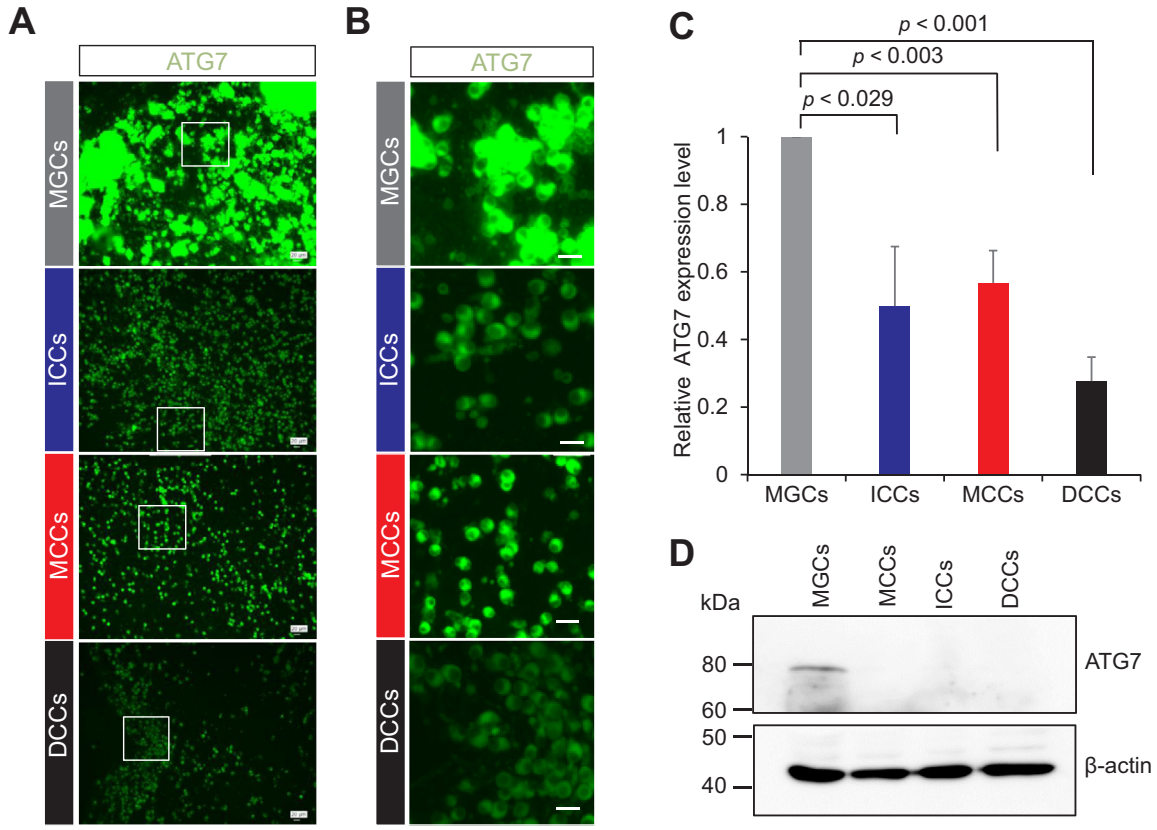


**Fig. 5. Expression of ATG proteins. A**, Immunostaining. Cells were stained with anti-human ATG7 antibody (green). Scale bar, 20 μm. **B**, Enlarged views of the white square regions in Fig. 3A. **C**, Quantification of fluorescent intensities of ATG7 proteins (over 300 cells were counted in each case). The expression level in MGCs was arbitrarily set at 1. The graph indicates relative ATG7 signal intensity against that in MGCs ($n = 3$). Values are expressed as mean ± SE. **D**, Immunoblotting with anti-ATG7 poly Ab. β-actin was immunoblotted as an internal control.

ml). When the follicles were stimulated as described previously [10], the serum estradiol level was 3266.7 ± 549.2 pg/ml before hCG administration. The mean number of retrieved oocyte from patients was 12.6 ± 1.5, and the fertilization rate was 6.6 ± 1.5%. When COCs obtained from patients were categorized by maturation stages, the average number was 6.2 ± 1.2 for mature COCs, 4.1 ± 0.6 for immature COCs, and 2.2 ± 0.4 for dysmature COCs.

After MGCs and COCs were isolated from the follicular fluid of patients, the oocytes were separated from COCs (Fig. 2A). The remaining cells were divided into three types of CCs, viz., immature and mature cumulus cells (ICCs and MCCs, respectively) and dysmature cumulus cells (DCCs) (Fig. 2B). The fertilization rate of oocytes separated from ICCs, MCCs, and DCCs was 53.8%, 60.7%, and 34.0%, respectively (Fig. 2C). The oocytes surrounded by DCCs exhibited significantly lower fertilization rate, compared with the oocytes surrounded by ICCs and MCCs. This result suggests that the physiological state of cumulus cells relates to oocyte quality. To understand the contribution of somatic cells surrounding the oocyte to the oocyte quality at the molecular level, we explored the characteristics of MGCs, ICCs, MCCs, and DCCs collected from these three types of COCs.

### 3.2. Subcellular localization of LC3 proteins

Autophagy is a self-eating mechanism in response to nutrient starvation by which cells destroy and rebuild cellular architectures [11]. Autophagy is generally assumed to serve as a survival mechanism for cells, and its deregulation links to non-apoptotic cell death [12]. Therefore, we supposed that autophagy may be involved in the quality control of somatic cells surrounding the oocyte. To address this issue, we immunocytochemically examined human granulosa and cumulus cells. The cells were immunostained with anti-LC3 polyAb, and nuclei were stained with DAPI. Of these cells, DCCs and MGCs exhibited remarkable immunoreaction with anti-LC3 polyAb, but fluorescent patterns were different between these cells (Fig. 3A). Although LC3 was diffusely localized in the cytoplasm of MGCs and DCCs, it appeared to be localized on intracellular structures such as nuclear membrane in DCCs. Our result suggests that excess LC3 expression is similar in MGCs and DCCs, but subcellular LC3 localization is distinct between these cells. Therefore, we assume that these cells may be classified under different situations.

### 3.3. DNA fragmentation

DNA fragmentation is a landmark of cell death and is observed in both apoptosis and non-apoptotic cell death [13,14]. To explore the relation of high expression of LC3 with cell death, we next examined the induction of DNA fragmentation. To detect DNA fragmentation, TUNEL assay was performed. TdT catalyzes the addition of dUTP nucleotides that have been labeled with biotin to the 3′-OH end of DNA strand breaks [15]. As shown in Fig. 3A, MGCs and DCCs were immunoreacted with anti-LC3 polyAb and their nuclei were labeled with TdT. Consistently, cleaved caspase 3 was detected only in MGCs (Fig. 3C and S2), indicating that apoptotic cell death occurs in MGCs, but not DCCs. The detection of DNA fragmentation discriminated ICCs and MCCs from DCCs and MGCs. Moreover, the fluorescent intensity of TdT labeling, corresponded to DAPI-labeled nuclear DNA, was higher in MGCs than that in DCCs (Fig. 3B), implying that the cellular condition may differ between MGCs and DCCs.

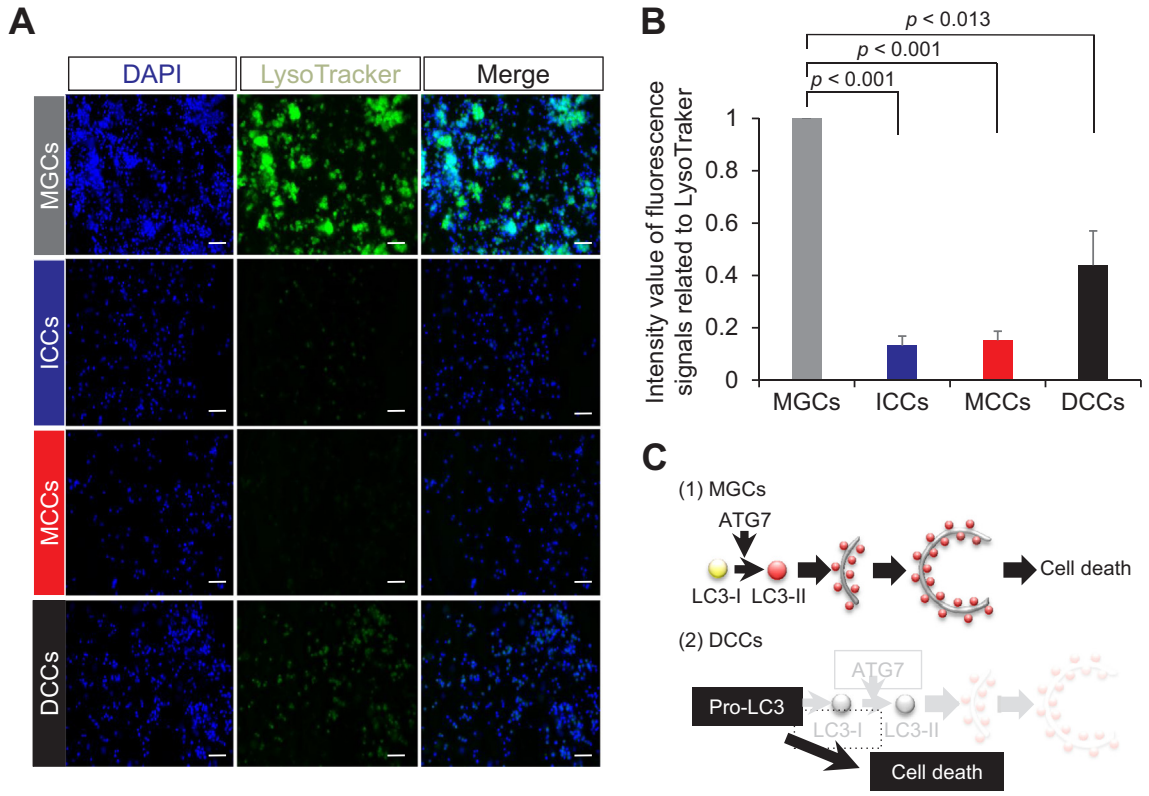


**Fig. 6. Lysosomal distribution. A**, Staining with LysoTracker. Cells were stained with LysoTracker Green DND26 (green) and counterstained for nuclei with DAPI (Blue). Scale bar, 50 μm. **B**, Quantification of fluorescent intensities of lysosomes (over 300 cells were counted in each case) ($n = 3$). The signal intensity in MGCs was arbitrarily set at 1. The graph indicates relative intensity value of fluorescence signals related to LysoTracker against that in MGCs. Values are expressed as mean ± SE. **C**, Hypothesis. (1) MGC death. Cell death is caused by autophagic cell death with participation of autophagosomes. (2) DCC death. Although expression of LC3 was detected in DCCs, no LC3-II signal was detected. Moreover, DCCs exhibited low ATG7 expression compared with that in ICCs and MCCs. Contrary to that observed for MGCs, DCC death may occur via an ATG7-independent mechanism.

### 3.4. Expression of LC3-I and -II proteins

To clarify the forms of LC3, we examined the expression of LC3 proteins by immunoblotting. At the initial stage of autophagosome formation, the LC3C-terminal fragment is cleaved to yield the cytosolic form LC3-I. The subpopulation of LC3-I is further converted to LC3-II, a membrane-bound, autophagosome-associating form. Here, we used a polyAb that recognizes both forms. β-Tubulin and GAPDH were used as internal controls. Our result showed that both LC3-I and LC3-II were detected only in MGCs and were below detectable level in all types of cumulus cells (upper panel, Fig. 4A and lower panel, 4B). When MGCs were incubated overnight in a serum-free medium, the levels of LC3-I and LC3-II proteins increased in response to nutritional starvation (upper panel, Fig. 4A).

The fluorescent signal with anti-LC3 polyAb was intense in DCCs (Fig. 3A), implying that an unprocessed form of LC3 (pro-LC3) may be detected (arrows of upper panel, Fig. 4A). To clarify expression pattern of pro-LC3 protein in detail, the amount of pro-LC3 proteins was densitometrically measured, and its value was normalized to that of GAPDH. When the amount of pro-LC3 in DCC was set to 100, pro-LC3 protein are totally abundant in MGCs and DCCs of patients (upper panel, Fig. 4B). However, the predicted pro-LC3 proteins were detected in DCCs, and their level was often very high in ICCs (patient #2) (upper panel, Fig. 4A and B), presumably indicating that DCCs are derived from ICCs. Proteins, with molecular weight of 55 kDa, corresponding to β-tubulin were recognized using an anti-β-tubulin mAb (middle panel, Fig. 4A). In addition, two lower molecular weight bands (40 and 28 kDa) were detected in all types of cells. Although β-III tubulin fragments inhibit neurodegeneration in neurons [16], the typical pattern and function of tubulin fragments are unknown in human granulosa cells. Thus, we assume that typical autophagy is initiated only in MGCs and atypical autophagy occurs or autophagy is arrested in DCCs.

### 3.5. Expression of ATG7 in human granulosa cells

Autophagy-related proteins (ATG proteins) primarily control autophagosome formation. In particular, ATG7 is an essential molecule for lipidation of LC3-I, which is converted to LC3-II [17]. If cell death occurs in DCCs in an autophagy-mediated manner, ATG7 should be expressed in DCCs. To clarify this possibility, we performed immunostaining with anti-ATG7 antibody. Although ATG7 expression was detected in all types of the cells examined, the fluorescence intensity of ATG7 in MGCs was significantly higher than that in DCCs (1 and 0.27 ± 0.07 in MGCs and DCCs, respectively; $P < 0.001$; Fig. 5A–C). ATG7 was also expressed in ICCs and MCCs, although the level of LC3 proteins was lower. Unexpectedly, it was demonstrated that the level of ATG7 proteins was the lowest in DCCs. Also, ATG7 was detected only in MGCs and under detectable level in other three types of cells (Figs. 5C and S3). From these results, we assumed that reduced ATG7 protein expression may lead to dysfunctional autophagy in DCCs.

### 3.6. Lysosomal proliferation

For complete degradation of accessory and damaged organelles, unification of lysosomes and autophagosomes is necessary [5]. Hence, we stained MGCs and CCs with LysoTracker Green DND-26 to estimate the number and distribution of lysosomes. Fluorescence signals related to LysoTracker were observed in MGCs and the DCCs (Fig. 6A). Moreover, the intensity was more remarkable in MGCs than that in the DCCs

(1 and 0.43 ± 0.13, respectively; $P < 0.013$; Fig. 6B). However, the fluorescence signals related to LysoTracker were very weak in ICCs and MCCs (Fig. 6A and B). These findings suggest that lysosome-mediated typical autophagy occurs in MGCs but not in DCCs.

## 4. Discussion

The physiological state of cumulus cells is associated with the oocyte quality, and determination of the physiological criteria of the CCs contributes to the diagnosis of infertility in patients. Here, we demonstrated the following points (Fig. 6C): First, the expression of LC3 proteins was significantly higher in MGCs and DCCs than that in ICCs and MCCs (Fig. 3A); Second, DNA fragmentation was strongly induced in MGCs and DCCs (Fig. 3A); Third, LC3 was produced from pro-LC3 proteins in MGCs but not in DCCs; Fourth, the expression of ATG7 proteins and number of lysosomes increased in MGCs but not in DCCs, indicating autophagy initiation (Figs. 5 and 6); Finally, lysosomal accumulation occurred in MGCs but in DCCs. Taken together, we propose that high expression of LC3 (presumably, pro-LC3) uncoupled with ATG7 expression and lysosomal abundance is useful as a biomarker to estimate lower quality of human cumulus cells.

Atg7 are prerequisite for induction of autophagy [18], and LC3 is a marker of autophagosomes [19]. Therefore, we believe that Atg7 and LC3 are essential for autophagy. Several studies have demonstrated that although LC3 is not detected in *Atg7*-deficient cells, autophagosomes are formed, suggesting the presence of an ATG7-independent pathway in autophagy [20,21]. These results imply that death of DCCs may occur through an Atg7-independent alternative atypical pathway.

In the present study, we explored the functional difference of autophagy according to the maturity of CCs surrounding the oocyte. First, the oocytes surrounded by DCCs showed significantly lower fertilization rate than ICCs and MCCs. Second, although pro-LC3 was highly expressed in MGCs and DCCs, the DCCs exhibited poor ATG7 expression and lower lysosomal accumulation, indicating the dysfunctional autophagy despite the intense expression of pro-LC3 proteins in DCCs. Based on these results, we concluded that the excess pro-LC3 expression overworks autophagy, and break autophagy-centric recycling system, resulting in entering cytotoxic unusual metabolites from CCs to oocytes presumably in gap junction-dependent manner, and lowering oocyte quality.

As shown in Fig. 3A, LC3 was localized in the cytoplasm of both MGCs and DCCs. Especially, the intense LC3 signal was observed in membranous structures in DCCs (Fig. 3A). On the other hand, both LC3-I and -II were undetectable in DCCs by immunoblotting (Fig. 4A). In other words, despite the absence of LC3-II, the membranous structures were intensely immunoreacted with anti-LC3 polyAb in DCCs, but not MGCs, implying that pro-LC3 may be accumulated on the membranous sturctures, presumably the nuclear membrane, but not autophagosomes, in DCCs. Because the expression patterns of LC3 and ATG7 were distinct between MGCs and DCCs, we assume that their physiological state may be different despite the same origin and similar morphology. In the ovarian cycle, immature follicles undergo degeneration or atresia, and these intricate processes are caused by apoptosis in granulosa cells during follicular development [22]. During follicular development, LC3 proteins are primarily detected in rat granulosa cells [22]. Consistent with this report, human MGCs also showed high expression of LC3 and ATG7 (Figs. 3 and 5). These results demonstrate that disabled autophagy in human granulosa cells is the main mode of cell death for follicular development.

However, autophagosomes are invisible in ovulated oocytes [7], and autophagy in the oocytes is suppressed by mammalian (or mechanistic) target of rapamycin complex 1 (mTORC1) [23]. After entering into the embryogenesis stage, autophagy in oocytes is induced and completed on fertilization with the sperm [8]. CCs probably protect the oocytes against autophagy inducers in the oviduct. To maintain the oocyte quality, CCs play an important role in suppressing autophagy in oocytes, which results in providing the most suitable environment for the oocytes. Our result support this hypothesis because all types of CCs showed completely decreased expression of ATG7 and distribution of lysosomes, which differed from that observed in MGCs (Figs. 5 and 6).

Because female reproductive processes, including ovulation and pregnancy, are controlled by a series of alterations of hormones, cytokines, and growth factors modulated by environmental and nutrition factors, examination on a single candidate may be insufficient and lead to misleading conclusions. Overall, our findings highlight distinct modes of cell death between MGCs and DCCs, which may be helpful to predict the state of CCs closely related to oocyte quality.

## Acknowledgements

This study was supported by a grant from the National Center for Child Health and Development, The Ministry of Health, Labour and Welfare, a Grant-in-aid for Scientific Research from The Ministry of Education, Culture, Sports, and Technology of Japan (#26670733 and #26293363).

## Appendix A. Transparency document

Supplementary data associated with this article can be found in the online version at doi:10.1016/j.bbrep.2018.08.002

## Appendix A. Supporting information

Supplementary data associated with this article can be found in the online version at doi:10.1016/j.bbrep.2018.08.002

## References

[1] G.W. Montgomery, S.M. Galloway, G.H. Davis, K.P. McNatty, Genes controlling ovulation rate in sheep, Reproduction 121 (2001) 843–852.
[2] M.A. Edson, A.K. Nagaraja, M.M. Matzuk, The mammalian ovary from genesis to revelation, Endocr. Rev. 30 (2009) 624–712.
[3] T. Yorimitsu, D.J. Klionsky, Autophagy: molecular machinery for self-eating, Cell Death Differ. 12 (Suppl. 2) (2005) 1542–1552.
[4] Y. Kabeya, N. Mizushima, T. Ueno, et al., LC3, a mammalian homologue of yeast Apg8p, is localized in autophagosome membranes after processing, EMBO J. 19 (2000) 5720–5728.
[5] P. Codogno, A.J. Meijer, Atg5: more than an autophagy factor, Nat. Cell Biol. 8 (2006) 1045–1047.
[6] M. Gaytán, C. Morales, J.E. Sánchez-Criado, F. Gaytán, Immunolocalization of beclin 1, a bcl-2-binding, autophagy-related protein, in the human ovary: possible relation to life span of corpus luteum, Cell Tissue Res. 331 (2008) 509–517.
[7] S. Tsukamoto, A. Kuma, N. Mizushima, The role of autophagy during the oocyte-to-embryo transition, Autophagy 4 (2008) 1076–1078.
[8] S. Tsukamoto, A. Kuma, N. Mizushima, et al., Autophagy is essential for preimplantation development of mouse embryos, Science 321 (2008) 117–120.
[9] R.D. Morais, R.G. Thomé, F.S. Lemos, N. Bazzoli, E. Rizzo, Autophagy and apoptosis interplay during follicular atresia in fish ovary: a morphological and immunocytochemical study, Cell Tissue Res. 347 (2012) 467–478.
[10] H. Saito, T. Kaneko, T. Takahashi, et al., Hyaluronan in follicular fluids and fertilization of oocytes, Fertil. Steril. 74 (2000) 1148–1152.
[11] L. Duprez, E. Wirawan, T. Vanden Berghe, P. Vandenabeele, Major cell death pathways at a glance, Microbes Infect. 11 (2009) 1050–1062.
[12] D. Gozuacik, A. Kimchi, Autophagy as a cell death and tumor suppressor mechanism, Oncogene 23 (2004) 2891–2906.
[13] D.J. Taatjes, B.E. Sobel, R.C. Budd, Morphological and cytochemical determination of cell death by apoptosis, Histochem. Cell. Biol. 129 (2008) 33–43.
[14] I.P. Nezis, B.V. Shravage, A.P. Sagona, et al., Autophagy as a trigger for cell death: autophagic degradation of inhibitor of apoptosis dBruce controls DNA fragmentation during late oogenesis in Drosophila, Autophagy 6 (2010) 1214–1215.
[15] Y. Gavrieli, Y. Sherman, S.A. Ben-Sasson, Identification of programmed cell death in situ via specific labeling of nuclear DNA fragmentation, J. Cell Biol. 119 (1992) 493–501.
[16] Y. Suzuki, C. Jin, T. Iwase, I. Yazawa, β-III Tubulin fragments inhibit α-synuclein accumulation in models of multiple system atrophy, J. Biol. Chem. 289 (2014) 24374–24382.
[17] Y. Ichimura, T. Kirisako, T. Takao, et al., A ubiquitin-like system mediates protein lipidation, Nature 408 (2000) 488–492.
[18] N. Mizushima, B. Levine, Autophagy in mammalian development and differentiation, Nat. Cell Biol. 12 (2010) 823–830.
[19] J. Wu, Y. Dang, W. Su, C. Liu, H. Ma, Y. Shan, Y. Pei, B. Wan, J. Guo, L. Yu, Molecular cloning and characterization of rat LC3A and LC3B-Two novel markers of

autophagosome, Biochem. Biophys. Res. Commun. 339 (2006) 437–442.
[20] M. Komatsu, S. Waguri, T. Ueno, et al., Impairment of starvation-induced and constitutive autophagy in Atg7-deficient mice, J. Cell Biol. 169 (2005) 425–434.
[21] Y. Nishida, S. Arakawa, K. Fujitani, et al., Discovery of Atg5/Atg7-independent alternative macroautophagy, Nature 461 (2009) 654–658.
[22] J.Y. Choi, M.W. Jo, E.Y. Lee, B.K. Yoon, D.S. Choi, The role of autophagy in follicular development and atresia in rat granulosa cells, Fertil. Steril. 93 (2010) 2532–2537.
[23] A. Yamamoto, N. Mizushima, S. Tsukamoto, Fertilization-induced autophagy in mouse embryos is independent of mTORC1, Biol. Reprod. 91 (2014) 1–7.